

# The evolution rate of quasars at various redshifts

Evanthia Hatziminaoglou, Ludovic Van Waerbeke, Guy Mathez

Observatoire Midi-Pyrénées, Laboratoire d'Astrophysique, UMR 5572, 14 Avenue E. Belin, F-31400 Toulouse, France

Received, , Accepted,

**Abstract.** The evolution of optically selected quasars is usually supposed to be well described by a single constant evolution parameter, either  $k_L$  or  $k_D$ , depending whether we refer to luminosity or density evolution. In this paper we present a study of the variations of the evolution parameters with redshift, for different cosmological models, in order to probe the differential evolution with redshift. Two different quasar samples have been analyzed, the AAT Boyle's et al. and the LBQS catalogues. Basically, these samples are divided in redshift intervals and in each of them  $k_L$  and  $k_D$  are estimated by forcing that  $\langle V/V_{max} \rangle = 0.5$ . The dependence with respect to the cosmological parameters is small. Both AAT and LBQS show roughly the same tendencies. LBQS, however, shows strong fluctuations, whose origin is not statistical but rather due to the selection criteria. A discussion on selection techniques, biases and binning effects explains the differences between these results. We finally conclude that the evolution parameter is almost constant in the redshift range  $0.7 \leq z \leq 1.7$ , at least within  $2\sigma$ , while it decreases slightly afterwards. Results depend on the binning chosen (but not in a very significant way). The method has been tested with Monte-Carlo simulated catalogues in order to give a better understanding of the results coming from the real catalogues. A correlation between  $k_L$  ( $k_D$ ) and  $\langle V/V_{max} \rangle$  is also derived and is used for the calculation of the error bars on the evolution parameter.

**Key words:** Cosmology: observational tests – Quasars: general, evolution

## 1. Introduction

Since the first application of the  $V/V_{max}$  test by Schmidt in 1968, the luminosity function of quasars is known to undergo a strong evolution, in the sense that the density of the most luminous quasars was far higher in the past.

*Send offprint requests to:* E. Hatziminaoglou, eva@obs-mip.fr

This was firstly interpreted in terms of either Pure Density (PDE - Schmidt, 1968) or Pure Luminosity Evolution (PLE - Mathez, 1976), and phenomenologically modeled with a single free parameter law. More complex models began to appear a few years later, such as a Luminosity Dependent Density Evolution (LDDE), proposed by Schmidt and Green in 1983. However, there wasn't any privileged model until the late 80's, when Boyle et al. (1988) favored PLE as a best fit of the observed luminosity function of a UVX sample. A similar recent result is found for X-Ray selected samples of quasars (Page et al. 1997; Jones et al., 1996; Boyle et al., 1993). The currently observed evolution of quasars appears however to be more complex nowadays, since the first indication of a reversing evolutionary trend around a redshift in the range [2.5,3] was observed (Shaver, 1994; Schmidt, Schneider and Gunn 1995; Warren, Hewett and Osmer 1994; Pei, 1995). A steepening of the luminosity function towards high redshifts is advocated by Goldschmidt and Miller (1997).

Meanwhile, the evolution of the cosmic star formation density was found to be strikingly similar to that shown by Shaver for QSOs, although the maximum of the star formation density is attained at a lower redshift (Madau, 1996). In spite of this difference, the similarity of the variations of QSO luminosity density and of the field galaxy star formation has been interpreted as a clue that both phenomena could be closely linked (Boyle and Terlevitch, 1998; Silk and Rees 1998). Furthermore, the similarity is even more striking (both curves have a maximum around the redshift  $z=2.5$ ) after applying the necessary correction for dust extinction in the density of high redshift galaxies (Shaver et al., 1998). This correction may be as high as a factor of ten since these galaxies are observed in their rest-frame ultraviolet.

In the same time, complex models of this evolution begin to appear:

- At high redshift, the growth of Dark Matter halos according to Press-Schechter formalism and the parallel Eddington-limited growth of accreting Massive Black Holes (MBH) (Haiman and Loeb, 1997) are likely to induce a decrease of density with increasing redshift ('neg-

ative DE') (Haiman and Loeb, 1997; Cavaliere and Vittorini, 1998; Krivitsky and Kontorovich, 1998; Novosyadlyj and Chornij, 1997).

- Around a redshift  $z=2.5$ , there could be two phenomena: a transition from high to low efficiency in advection-dominated flows, followed by the decline of accretion rate, giving luminosity proportional to  $(1+z)^k$  with  $k$  slightly variable around 3 (Yi, 1996). Alternatively, growing galaxies could assemble in groups of typically  $5 \cdot 10^{12} M_{\odot}$ , where tidal effects refuel the MBH at lower and lower rate, translating into 'positive LE' (Cavaliere and Vittorini 1998).

- At intermediate redshift, viscous instabilities induce long term, high amplitude variations of the accretion rate. The fraction of time spent at each luminosity level, convolved with the mass distribution gives the luminosity function and its evolution (Siemiginowska and Elvis, 1997). Galaxy collisions provide a mechanism which fuels galactic nuclei with gas in dense environments, giving raise to quasars in low luminosity galaxies (Lake, Katz and Moore, 1997).

- In addition, gravitational lensing mimics luminosity evolution in flux-limited samples, amplifying the more distant quasars, but whose detailed effect is not known, in particular the induced bias selection effects in magnitude limited quasar samples.

Van Waebeke et al. (1996) define a new test, the  $V/V_{max}$  statistics, and apply it to the AAT quasar sample (Boyle et al., 1990). They show that, contrary to the usual  $\langle V/V_{max} \rangle$  test, the  $V/V_{max}$  statistics leads to constraints on cosmological parameters. However these results rely on an arbitrary model of PLE, since the evolutionary effects dominate the cosmological effects in the QSO distribution, and we have to be sure of the reliability of the evolution model before constraining the cosmological parameters. So, the analysis in Van Waebeke et al. (1996) is rather a test of compatibility between an evolution model and a couple of cosmological parameters and there is a need for an *independent* better understanding of the QSO evolution before applying such cosmological tests.

A number of projects aim at assembling complete and homogeneous samples of several thousands of quasars which will allow more reliable and more subtle analyses, leading, thus, to verifications or improvement of complex theories on quasar evolution.

Finally, there is some hope for progress in the understanding of the evolution of the stellar formation rate and of quasars, and in the determination of cosmological parameters compatible with the observed quasar distribution. Note that this is a necessary framework in order to make a precise estimate of the effects of the re-ionization in the future temperature maps of Planck-Surveyor.

The aim of this paper is to explore in details the possibility for the evolution to depend on the redshift, and on whether we can distinguish between artefact and physical evolution. For the present study we decided to adopt a cosmology and an evolution model with a single evolu-

tion parameter which is allowed to depend on the redshift (and/or the magnitude in Section 4). This should lead to more complex evolution laws, which may help in theoretical understanding of quasar evolution and in turn could be the basis of future, more realistic cosmological tests.

The technical basis of this work is the  $\langle V/V_{max} \rangle$  test, performed in bins of redshift. In §2 and 3 we make a brief description of the quasar samples and the evolution models used. In §4 we give a justification of our choice to study quasar evolution in redshift bins and in §5 we present the different redshift binning modes used for our study. §6 contains the results obtained from the simulated catalogues. §7 contains the results for the real quasar samples. More precisely, it shows the measured dependence of the evolution parameter versus redshift, for a few sets of cosmological parameters. Finally, in §8 we discuss the main results of our study.

## 2. Samples used

In this study two complete quasar samples have been used, the AAT catalogue of Boyle et al. (Boyle et al., 1990) and the Large Bright Quasar Survey catalogue (Hewett et al., 1995), hereafter AAT and LBQS respectively. The AAT catalogue contains 400 faint quasars selected by their UV excess, it is claimed to be complete within  $18 \leq m \leq 21$  and  $0.2 \leq z \leq 2.29$ . LBQS consists of 1055 optically selected quasars of intermediate brightness, with  $16.5 \leq m_{BJ} \leq 19$ , within the redshift range  $0.2 \leq z \leq 3.4$ . Various methods have been used for the selection of this catalogue, combining a color selection technique and slitless spectroscopic data. LBQS is almost three times bigger in size and much more profound in redshift than AAT, but its selection criteria depend on the redshift. This means that the selection biases differ from one bin of redshift to another, which will lead to dramatic effects on the measured evolution. In the case of AAT, the UVX selection technique applied in the whole redshift range insures the fact that the biases can be comparable throughout the whole sample. The differences between the two samples may influence the results on quasar evolution thus a direct comparison may not be possible.

## 3. Evolution models and evolution parameter

### 3.1. PLE and PDE

In order to explain the observed non-uniform spatial distribution of quasars, several empirical evolution models have been proposed such as the PLE (Pure Luminosity Evolution) model, the PDE (Pure Density Evolution model) and the LDDE (Luminosity Dependent Density Evolution). In this paper, we will make an extensive use of PLE and PDE, whose introduction was purely phenomenological. PLE makes the hypothesis of a constant

object space density and supposes the following form for the luminosity:

$$L(z) = L(0)e(z) \quad (1)$$

where  $e(z)$  is an one parameter evolution law. On the contrary, PDE assumes a constant quasar luminosity and a redshift–dependent space density:

$$\rho(z) = \rho(0)e(z) \quad (2)$$

### 3.2. Power Law and Exponential Parametrizations

The most commonly used expressions for  $e(z)$  are the power law form

$$e(z) = (1 + z)^k \quad (3)$$

and the exponential form

$$e(z) = \exp(k \tau(z)) \quad (4)$$

where  $\tau(z)$  is the lookback time, and  $k$  is the evolution parameter ( $k_L$  and  $k_D$  in the cases of a PLE and a PDE, respectively).

The basis of this work is the  $\langle V/V_{max} \rangle$  test, or rather the  $\langle V_e/V_a \rangle$  test (Avni and Bahcall, 1980), with all volumes computed according to Mathez et al., 1996.

In the following we examine the variations of the evolution parameter in magnitude and redshift bins for PLE and PDE models. All  $k_L$  ( $k_D$ ) calculated here are the optimum values which insure a  $\langle V/V_{max} \rangle = 1/2$  ( $\langle W/W_{max} \rangle = 1/2$ )<sup>1</sup> within each bin, a necessary (but not sufficient) condition for a uniform  $V/V_{max}$  ( $W/W_{max}$ ) distribution within the interval  $[0, 1]$ . The dependence of  $k_L$ 's ( $k_D$ 's) versus redshift is measured and all calculations are made for several cosmological models. During our work, we examined cosmological models with  $\Omega_0$  and  $\Lambda$  varying between 0 and 1 with steps of 0.25. In the present paper we chose to demonstrate our results for the flat universes cosmological models ( $\Omega_0 + \Lambda = 1$ ), excluding the rather non-realistic model  $(\Omega_0, \Lambda) = (0, 1)$ . In all plots representing  $k_L$  or  $k_D$  versus  $z$ , the values of the evolution parameter increase with increasing  $\Omega_0$  and with decreasing  $\Lambda$ , unless specified otherwise. So the lower curve corresponds to the model  $(\Omega_0, \Lambda) = (0.25, 0.75)$  while the upper one to the model  $(\Omega_0, \Lambda) = (1.0, 0.0)$ . The above method allows a direct determination of the evolution parameter error bars; the  $1\sigma$  region of  $\langle V/V_{max} \rangle$ , calculated assuming no evolution, is given by  $1/2 \pm 1\sigma$  with  $\sigma = (\sqrt{12N})^{-1}$ , where  $N$  is the number of quasars within each bin. A corresponding error bar on the evolution parameter can thus be derived from this  $1\sigma$  interval of  $\langle V/V_{max} \rangle$ . We will go back to this point in the Appendix.

Our method differs significantly from that used by Boyle et al., 1988 on the AAT sample. They showed that

PLE power law with  $k_L \simeq 3.5$  is a good fit to the AAT sample, with a technic which consists in calculating the luminosity function within redshift bins and in fitting the results to a luminosity function model. This method has the drawback to consider the evolution parameter as a free adjustable parameter, as well as the slopes of the luminosity function, the density, and the absolute magnitude linking the two slopes. It does not take into account the physical information that the quasars should be uniformly distributed, once the evolution has been corrected. Indeed, this information allows the evolution parameter to be determined directly from a  $V/V_{max}$  test without any hypothesis on the luminosity function.

## 4. Evolution in bins of magnitude

### 4.1. Apparent magnitude

In case of PLE it is very difficult to divide a sample in bins of absolute magnitude, even through complex methods, because absolute magnitude has to be estimated at a given epoch and thus depends on the evolution law. On the contrary, a division in bins of apparent magnitude,  $m$ , is very easy to operate. The AAT sample has been divided into 5 bins which contain equal numbers of quasars. In Fig. 1 we present the evolution parameter  $k_D$  versus  $m$  under a power law hypothesis. We notice a diminishing trend up to  $m \simeq 20.5$  reversing towards fainter magnitudes. This trend can be a priori understood in terms of variations of evolution with either redshift or absolute magnitude since both are more or less correlated with apparent magnitude.

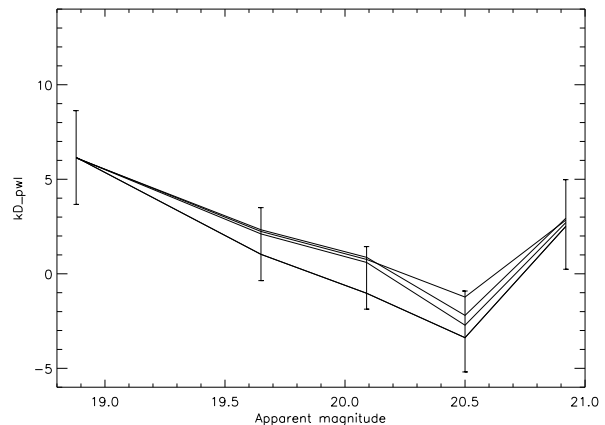


**Fig. 1.** Variations of the evolution parameter  $k_D$  with apparent magnitude for flat universe cosmologies, with a power law evolution model. The different curves correspond to the different cosmological models specified in the text.

<sup>1</sup>  $W(z)$  is defined as:  $dW(z) = \rho(z)dV(z)$

#### 4.2. Absolute magnitude

Analyzing a sample of quasars with a PDE hypothesis, and with  $M_0 < -23$  for the cosmological models with  $q_0 = 0.1$  and  $q_0 = 0.5$ , Schmidt and Green (1983) derived that the evolution parameter  $k_D$  increases with absolute magnitude. Making a similar analysis on AAT and LBQS catalogues (which span a larger absolute magnitude range), we find no clear tendency for the evolution parameter  $k_D$  versus absolute magnitude, whatever the cosmological model used. The samples have both been divided in 5 bins of absolute magnitude with a constant number of objects ( $\sim 80$  for AAT,  $\sim 210$  for LBQS). Fig. 2 illustrates the results for the zero curvature cosmological models examined above. On the right side of the figures we present a typical error bar. Note that the scaling of the vertical axis is the same in both Figs. 1 and 2.

From this previous analysis, we conclude that Fig. 1 could reflect a redshift dependence, not an absolute magnitude effect, and that is why this paper is devoted to the redshift dependence of the evolution.

### 5. Bins of Redshift

The quasar samples have been divided into several redshift bins in order to examine the redshift dependence of the evolution parameter and the influence of the cosmological model. The AAT analysis is limited to the redshift interval  $[0.3, 2.2]$ , because, at low and high redshift, the sample is obviously not complete. The binning intervals are defined here.

The binning was chosen so as to be optimized with respect to different criteria. The first one is that bins should contain a sufficient number of quasars in order to make a reliable statistical analysis. The second one is that they should be narrow enough so that the evolution parameter may be considered as constant within a single bin. The third criterion is that, according to the parametrization of the evolution hypothesis, we must chose the binning in order to distribute the amount of evolution equally within bins.

Our first choice of binning insures equal numbers of quasars, in order to distribute equally the statistical noise between bins and to minimize it, thus satisfying the first criterion above. The AAT sample was divided in 5 bins of about 80 quasars each (binning (B1), Table 1) while the LBQS sample was divided in 11 bins each one containing about 100 quasars. Redshift limits for LBQS are: 0.20, 0.37, 0.57, 0.75, 0.96, 1.14, 1.36, 1.81, 2.10, 2.52, 3.36.

We must be sure however that the variations of the observed evolution we are looking for are not biased by the binning chosen. It could be the case if the evolution rate differed too much from bin to bin. This is why, for each assumed evolution law  $e(z)$ , we look for a binning ensuring equal ratios  $e(z_{i+1})/e(z_i)$ . In the case of a power law parametrization for example, used to describe most of

the evolution laws derived for quasars, the redshift enters through the factor  $(1+z)^k$  (see equation 3). With such a law and binning (B1) in Table 1, the ratio  $\left(\frac{1+z_{i+1}}{1+z_i}\right)^k$  which governs the evolution rate within bin  $i+1$ , decreases strongly from bin to bin and this is likely to bias the analysis. If we want to take into account the dependence of the evolution rate with redshift, we must impose the redshift intervals' limits,  $z_i$ , such as:

$$\frac{1+z_{i+1}}{1+z_i} = \frac{1+z_{i+2}}{1+z_{i+1}} \quad (5)$$

With this binning (B2), the evolution should be comparable within all bins and we should be expecting a somehow more uniform  $\langle V/V_{max} \rangle$  distribution, provided that  $k$  does not vary too much from bin to bin.

**Table 1.** Bins' redshift limits and quasar numbers for AAT sample. The  $z_i$  for the third binning have been computed for the cosmological model  $(\Omega_0, \Lambda) = (0.5, 0.5)$ .

(B1)	$z_i$	0.30	0.86	1.22	1.57	1.87	2.2
	$n$		78	78	78	78	78
(B2)	$z_i$	0.30	0.56	0.86	1.23	1.67	2.2
	$n$		19	66	72	104	124
(B3)	$z_i$		0.30	0.51	0.80	1.27	2.2
	$n$			15	47	99	222

The exponential parametrization leads to another binning, also given in Table 1 (binning (B3)) for the cosmological model  $(\Omega_0, \Lambda) = (0.5, 0.5)$ . Here, the look-back time intervals are constant within bins (note that the bins' limits depend slightly on the cosmological model). We chose to divide the sample in 4 bins because of the very small numbers of quasars contained in the first two bins in a choice of a division in 5 redshift intervals (13 and 33). We remind the reader that a high number of quasars within bins is very important because of the statistical nature not only of the test, but of the evolution itself, which is a further motivation for large redshift bins. But too large a bin may bias the evolution parameter estimation if the evolution rate changes too strongly with the redshift, which may be the case in the last redshift interval for this binning.

### 6. Tests with simulated catalogues

The method has first been validated with Monte-Carlo simulated catalogues. The aim of these tests was to examine the results obtained by analyzing simulated catalogues, constructed under specific hypotheses for the whole redshift interval, whose properties are *a priori* known. Here

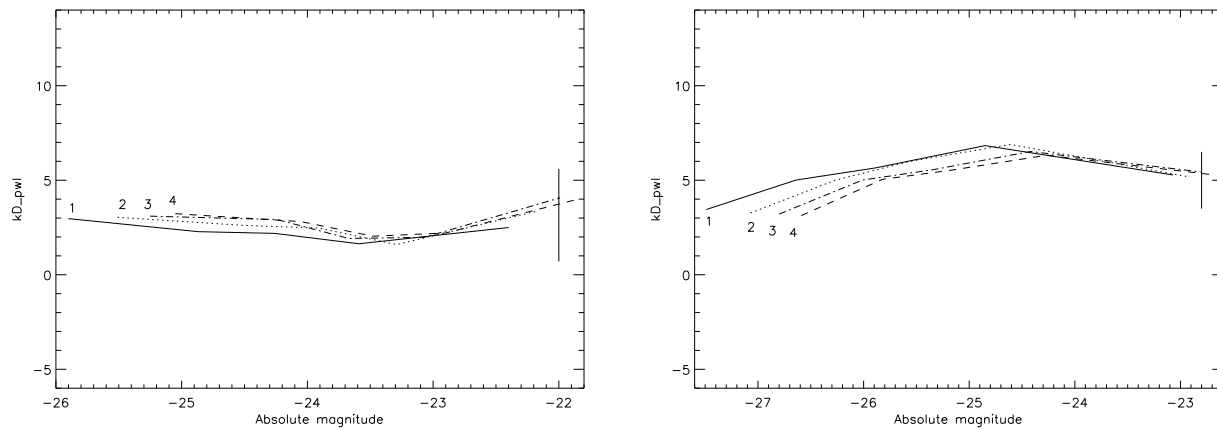


**Fig. 2.** LDDE for a power law evolution model, for AAT (left) and LBQS (right): variations of the evolution parameter  $k_D$  with absolute magnitude for 4 flat universe cosmological models: 1)  $(\Omega_0, \Lambda)=(0.25, 0.75)$ , 2)  $(\Omega_0, \Lambda)=(0.5, 0.5)$ , 3)  $(\Omega_0, \Lambda)=(0.75, 0.25)$  and 4)  $(\Omega_0, \Lambda)=(1.0, 0.0)$ . There is no clear trend for  $k_D$  with absolute magnitude. The bar on the right gives the error bar's size ( $1\sigma$ ).

we present two different tests applied to simulated catalogues whose characteristics mimics the properties of AAT. The details of the simulation algorithm can be found in Mathez et al. 1996.

For the first test, 38 simulated catalogues of 400 quasars each, were built under a constant luminosity evolution hypothesis, a power law parametrization with  $k_L = 3.47$ , within the redshift region  $z \in [0.3, 2.2]$ . The cosmological model used for the construction was  $(\Omega_0 = 0.5, \Lambda = 0.5)$ . Fig. 3 shows the measured evolution in redshift bins (with the binning B2) on these catalogues. The solid line indicates the true value  $k_L = 3.47$ , the dashed-dotted line includes the 68% of the values and the dashed line corresponds to the variations of the median  $k_L$  value with redshift. The analysis with binning (B1) on the same catalogues gives a similar result, which proves that for a constant evolution rate, the method is not sensitive to the chosen binning.

For the second test, 44 simulated catalogues were build under a PLE, exponential parametrization ( $k_L = 5$ ), for the same cosmological model as above. The analysis has been made for binning (B3) and assuming a (wrong) PDE hypothesis. The results on Fig. 4 shows that a density evolution is measured, with  $k_D$  slightly lower than the true  $k_L$ . It should not be surprising, indeed with a  $V/V_{max}$  method, it is impossible to separate luminosity and density evolution. On the contrary, the distinction between these two kinds of evolution is possible with methods based on luminosity function hypothesis (as in Boyle et al., 1988), but as explained in Section 3, it suffers from some other problems.

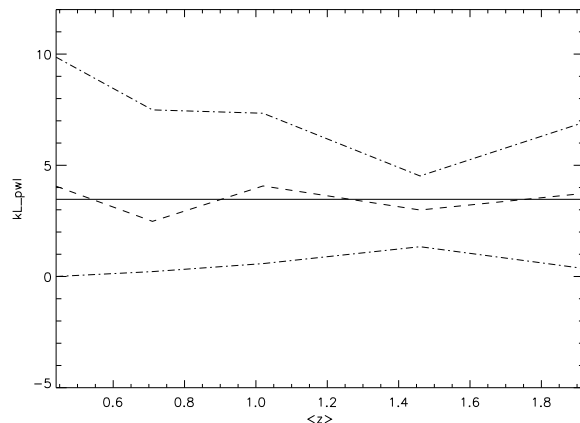


**Fig. 3.**  $k_L$  versus  $z$  for 38 simulated catalogues, binning B2. The dashed-dotted line includes the 68% of the  $k_L$ 's values, while the dashed line illustrates the variations with redshift of the median value. All catalogues were constructed under a PLE, power law hypothesis of  $k_L = 3.47$  for the cosmological model  $(\Omega_0, \Lambda) = (0.5, 0.5)$ .

## 7. Evolution parameter versus $z$

The evolution parameter is now calculated within each redshift bin, by forcing that  $\langle V/V_{max} \rangle = 0.5$  (or  $\langle W/W_{max} \rangle = 0.5$ ). An error bar is also derived, from the  $1\sigma$  interval of  $V/V_{max}$ , according to the method described in details in the Appendix.

### 7.1. PLE results

Fig. 5 shows  $k_L(z)$  for AAT catalogue for power law and exponential forms, and zero curvature cosmological models. Binning (B1) is the first to be examined.

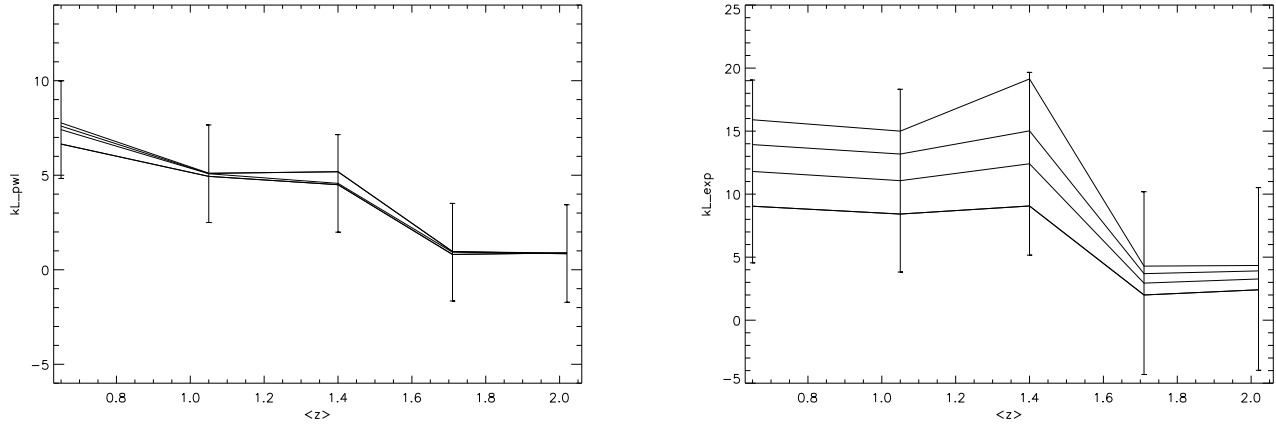


**Fig. 5.** AAT: The sensitivity of  $k_L$  to cosmological models and its variations with redshift, for equally populated bins (binning B1), for a power law parametrization (left graph) and the exponential parametrization (right graph). The models treated are those with zero curvature.

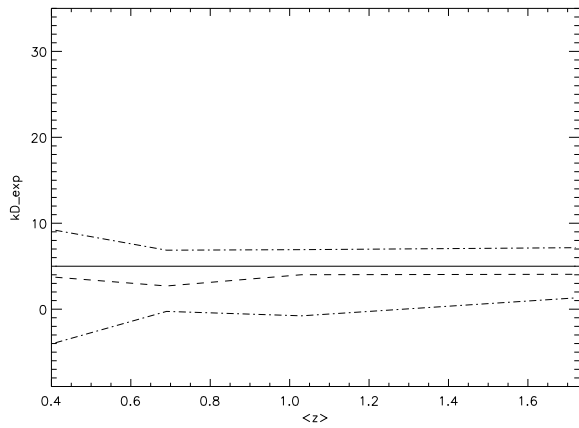


**Fig. 4.**  $k_D$  versus  $z$  for 44 simulated catalogues, binning B3. The dashed–dotted line includes the 68% of the  $k_D$ 's values, while the dashed line illustrates the variations with redshift of the median value. All catalogues were constructed under a PLE, exponential law hypothesis of  $k_L = 5$  for the cosmological model  $(\Omega_0, \Lambda) = (0.5, 0.5)$ , and analysis is made under PDE exponential law hypothesis.

The left plot corresponds to a power law and the right one to the exponential law parametrization. In both cases  $k_L$  decreases slightly with redshift. The same analysis on the LBQS (Fig. 6), results in a figure dominated by strong fluctuations, absent in the result given by the AAT (Fig. 5). The fact that AAT and LBQS have not the same magnitude range is not enough to explain why the evolution is so different between these two catalogues. Fig. 6 also shows a global decreasing trend of  $k_L$  with increasing redshift, which is marginally significant accounting for the error bars.

The reason for this discrepancy should first be searched in the incompleteness and/or the selection bias of the catalogues, in particular in the LBQS which has a complex selection criteria. The combination used (hypersensitized IIIa-J+GG395) had a maximum width of 2000 Å with a maximum response at a wavelength of around 4200 Å and a blue limit imposed by the atmospheric cut-off at  $\sim 3200$  Å while the red one was due to the emulsion. Objects either with a detected emission line or whose median wavelength of the SED was found bluewards of the central wavelength were classified as quasar candidates while the others were rejected (Hewett et al., 1995). The most intense emission lines of quasars in the waveband we are interested in along with their relative intensities are listed in Table 2.

**Table 2.** Quasars' strong emission lines and relative intensities taken from current literature.

Emission line	wavelength (Å)	relative intensity
Ly $\alpha$	1216	1
CIV	1549	0.5
CIII]	1909	0.2
MgII	2798	0.2

As redshift increases, the quasar strong emission lines appear successively in the blue and in the red part of the LBQS spectral range, leading each time to a shift of the median wavelength. This gives rise first to an excess and then to a deficiency of quasar candidates. Fig. 7 gives our estimation on this effect on the detection rate, and finally in the evolution parameter  $k_L$ . We estimated that the filter's response gets its maximum value at a wavelength of

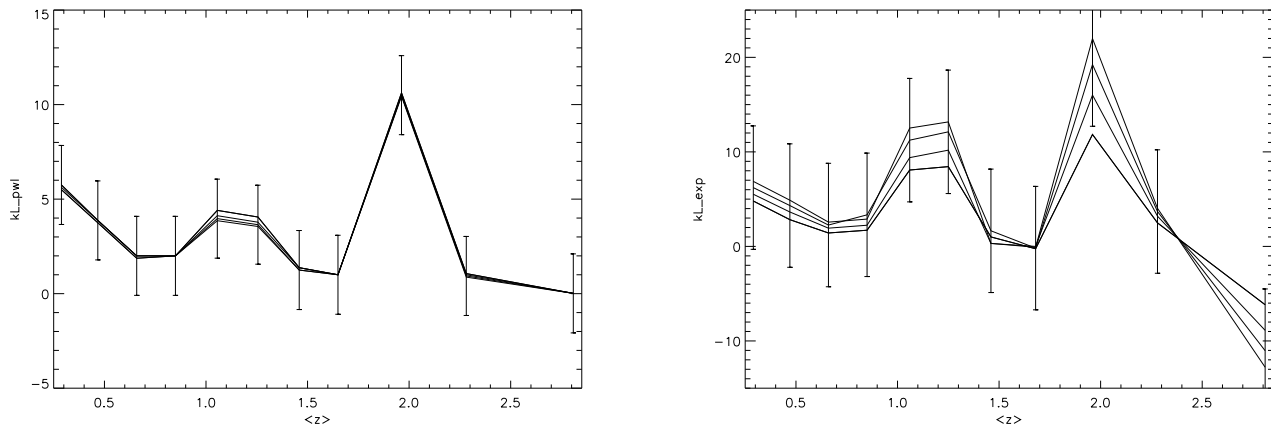


**Fig. 6.** The sensitivity of  $k_L$  to cosmological models and its variations with redshift for the LBQS analysis in equally populated bins (binning B1). The left graph corresponds to a power law hypothesis; the right one to an exponential form. The models treated are those with zero curvature. The fluctuations seen above are most probably due to the passage of strong emission lines through the filter's mean wavelength.

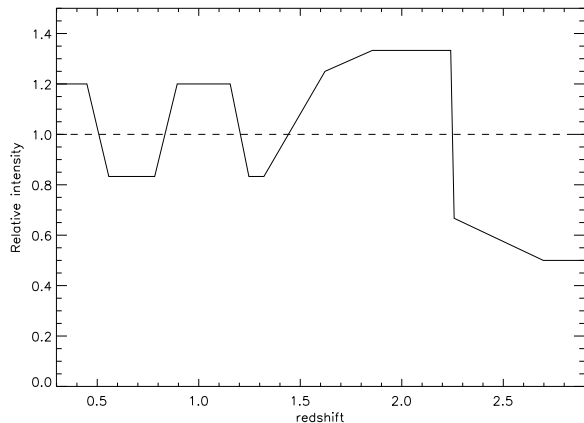


**Fig. 7.** Relative excess and deficiency of apparent evolution due to strongest emission lines in the LBQS.

$\sim 3700 \text{ \AA}$  and that it remains almost constant up to a  $\lambda \sim 4900 \text{ \AA}$ . Based on these hypotheses we first calculated the redshift regions where each emission line would contribute to an excess (and to a deficiency) depending on its relative intensity. The conversion of wavelengths to redshifts has been made by using the forms:

$$(\lambda_L + \Delta\lambda_L)(1 + z_{1L}) = \lambda_1 \quad (6)$$

$$(\lambda_L \pm \Delta\lambda_L)(1 + z_{2L\pm}) = \lambda_2 \quad (7)$$

$$(\lambda_L - \Delta\lambda_L)(1 + z_{3L}) = \lambda_3 \quad (8)$$

with  $\lambda_1 = 3700 \text{ \AA}$ ,  $\lambda_2 = 4200 \text{ \AA}$  and  $\lambda_3 = 4900 \text{ \AA}$ ,  $\lambda_L$  the wavelengths given in Table 2 and  $\Delta\lambda_L$  the Full Width Half Maximum (FWHM) of each line.  $z_{1L}$  is the redshift at which the emission line  $L$  enters the detection

range, contributing to an apparent quasar excess.  $z_{2L+}$  marks the end of this contribution. At  $z = z_{2L-}$  the emission line enters the filter's red region and causes an apparent deficiency of objects and after  $z_{3L}$  it is no longer detectable. As FWHM and EW vary from one quasar to the other and from one emission line to the other, approximate values have been used, taken from Ulrich, 1989. The composition of Fig. 7 (whose similarity with Fig. 6 is obvious), has been made by superimposing the results for the 4 emission lines. The  $k_L$ 's maxima approximately coincide with the probable high detection rate points giving a possible explanation for the  $k_L$ 's fluctuations with mean redshift. According to Hewett et al. (1995), other factors are likely to influence also the quasars' detection rate but their analysis is outside the aims of this paper.

Right afterwards we test binnings (B2) and (B3) for AAT sample. Fig. 8 shows the variations of  $k_L$  with redshift  $z$  for these two cases. The values of  $k_L$  are almost constant within error bars in the redshift range  $0.7 \leq z \leq 1.7$ . However, the values of  $k_L$  in small redshift bins are not very reliable, as we can see from the first error bar in both graphs, due to the very small number of quasars (see Table 1). We repeated the procedure described above but this time we divided the sample into 4 bins, so as to have more objects (32) in the first bin. We found that the evolution parameter was significantly higher in this bin and constant in the others but we cannot use these results: because of the large size of the three other redshift intervals, the test loses its sensitivity. From the above we conclude that a PLE (or a PDE as shown later on), with  $k_L \simeq 3.5$  for a power law and  $k_L \simeq 9$  for an exponential, fits the sample, as already demonstrated by Boyle et al. (1988) (but our method differs significantly, as explained in Section 3.2). We also applied the analysis to LBQS for the equivalent of binnings (B2) and (B3) as well as for random binnings,

even though we consider this sample as highly biased. We find in average no significant decrease of  $k$  with increasing  $z$ , up to  $z \simeq 2$ . Fig. 9 illustrates these results for binning (B2). Peaks are far less intense but excess and deficiency are found in the predicted places (compare with Fig. 7).

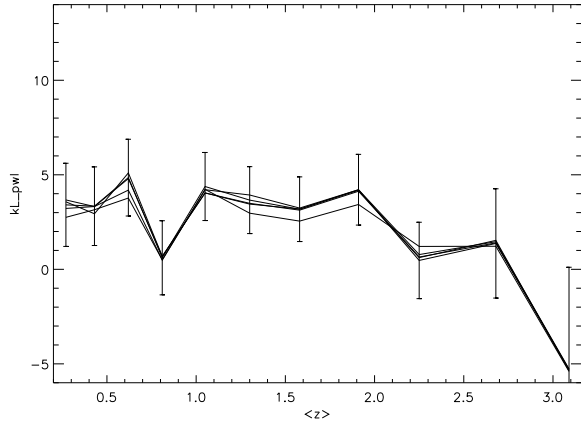


**Fig. 9.**  $k_L$  variations with redshift for LBQS, for binning (B2).  $k_L$  is rather constant within the redshift range  $0.3 \leq z \leq 2$ .

### 7.2. PDE results

The same work has been made under the hypothesis of a PDE, for both power law and exponential laws. In Figs. 10 and 12 we present the results for AAT for the three binnings and in Fig. 11 the results for LBQS for the first binning.

In all cases we find the same characteristics and the same trends as for the PLE hypothesis. As already mentioned in Section 6 about the simulated catalogues, a density evolution almost as strong as a luminosity evolution is measured because of the degeneracy between these two kinds of evolution, which is not broken by the  $V/V_{max}$  method. All figures concerning binning (B1) for AAT point out that whatever the hypothesis on the evolution law, the evolution parameter declines slightly with redshift. The similarity between the results of the PLE and PDE hypotheses indicates that both evolution models fit equally AAT sample. In the case of LBQS the evolution parameter's peaks become less intense but they are always present.

Furthermore, the small variations with redshift of  $k_L$  and  $k_D$  imply that both models, when assuming a constant evolution parameter, are not far from being correct, at least in the redshift range  $[0.7, 1.7]$ . With binning (B1) for AAT however, the picture (Fig. 5 and 10) was rather of a regular decrease of the evolution parameters with increasing  $z$ . In order to check this point we made the same analysis in a series of random binnings, for both AAT and LBQS. We found that most binnings rather point to a

constant evolution parameter, at least up to  $z = 1.7$  and to a small tendency towards a regular decrease above this redshift.

### 7.3. Summary

We will now give a different representation of our results concerning AAT, by calculating the relative luminosity and density, normalized at  $z = 2.2$ , for both PLE and PDE models. Fig. 13 illustrates  $\log L(z)/L(2.2)$  (solid lines) and  $\log \rho(z)/\rho(2.2)$  (dashed lines) versus  $z$ . Diamonds and squares correspond to binning (B1) given in Table 1, for a power law parametrization. Triangles and stars correspond to binning (B2), for the same parametrization. The two curves without symbols represent the third binning, (B3), and an exponential parametrization. Error bars have been plotted for each binning. As it may be noticed, they become wider as the redshift is smaller because of the propagation of errors in the calculation of the normalization constants. All calculations have been made for the  $(\Omega_0, \Lambda) = (0.5, 0.5)$  model. There is a remarkable similarity with previous results (see e.g. Fig. 7 of Shaver (1994), Fig. 3 of Pei (1995) and Fig. 1 of Shaver et al., 1998, all obtained from different procedures) as well as with the theoretical results of Yi (1996, Fig. 2). In the inset figure we present the same quantities calculated for a constant evolution parameter. The solid line represents a power law parametrization of  $k = 3.5$  while the dashed line represents an exponential parametrization of  $k = 9$ .

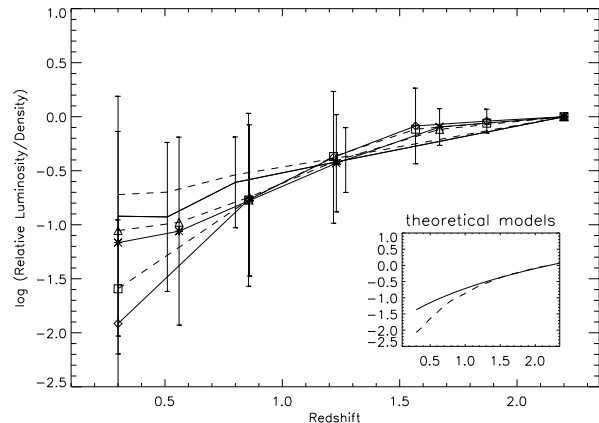


**Fig. 13.** Relative Luminosity (solid lines)/density (dashed lines) normalized to  $z = 2.2$  versus  $z$ .  $\square, \diamond$ : (B1), power law parametrization.  $\triangle, *$ : (B2), same parametrization. Lines without plotting symbols: (B3), exponential parametrization. Inset figure: the solid line represents a power law parametrization of  $k = 3.5$  while the dashed one represents an exponential parametrization of  $k = 9$ .



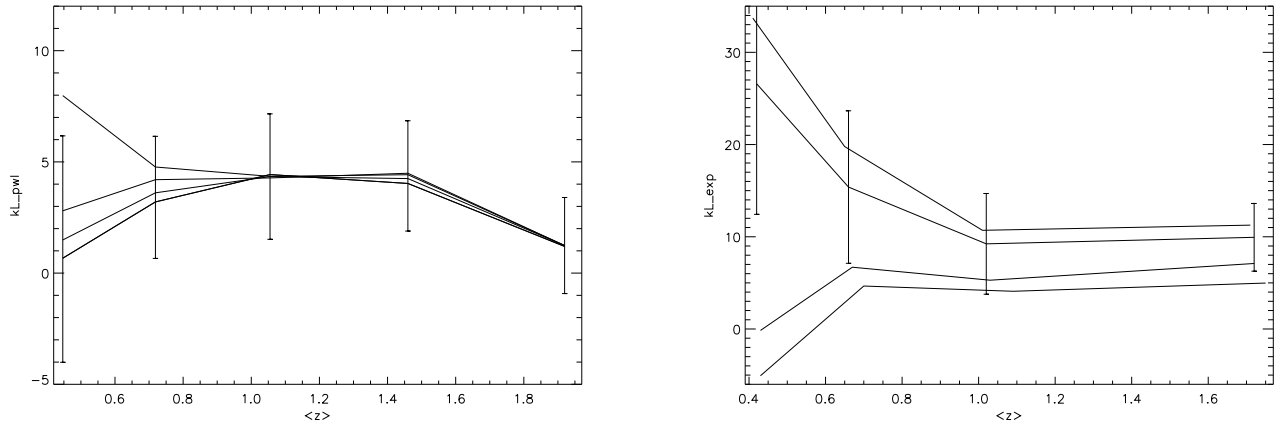


**Fig. 8.**  $k_L$  variations with  $\langle z \rangle$  for AAT, for flat universe models and for binning B2 given by equation 5 (left graph) and for binning B3 ensuring equal look-back time intervals (right graph). (Note the difference of the scales of the vertical axis on the two graphs.)

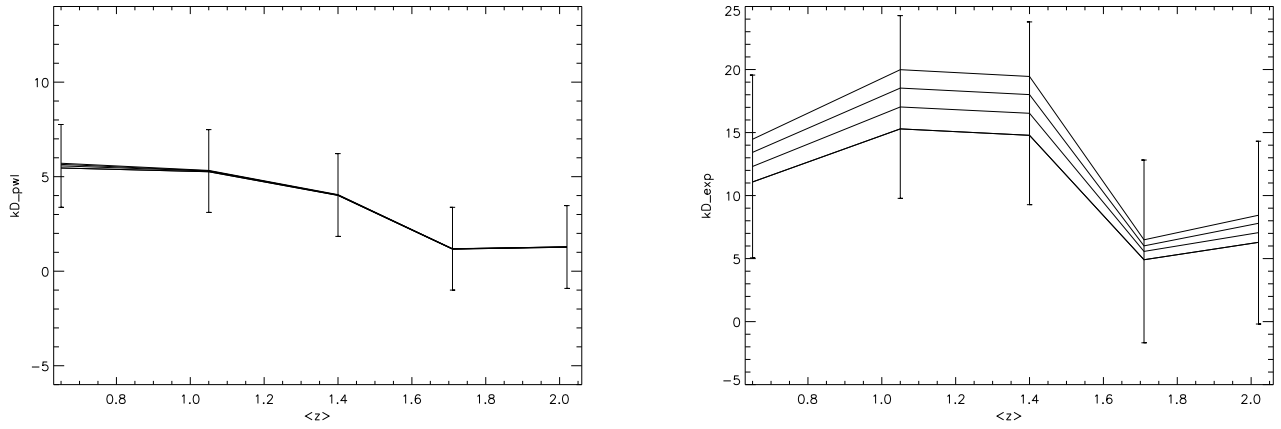


**Fig. 10.**  $k_D$  versus  $\langle z \rangle$  for AAT catalogue, binning B1. Left graph: power law PDE, right graph: exponential PDE.

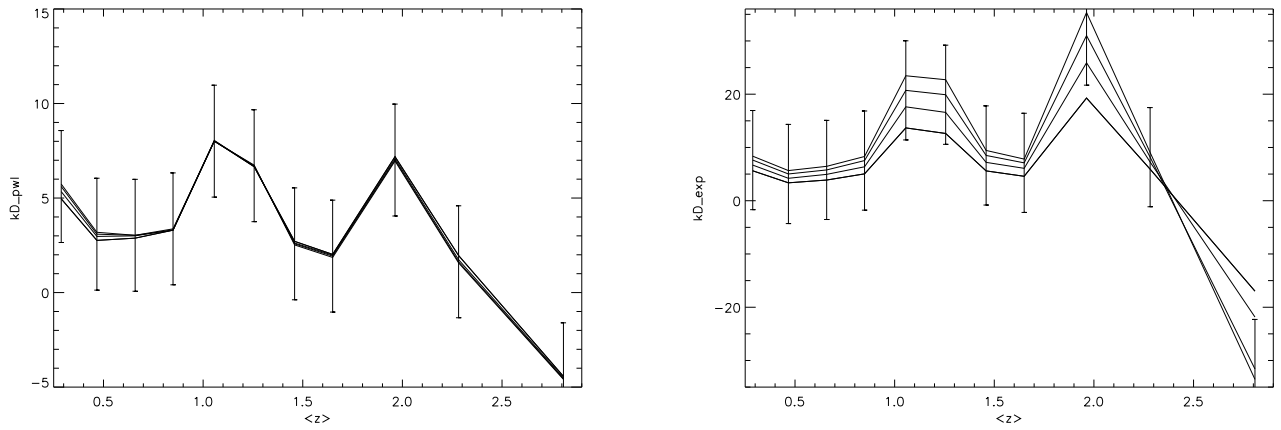


**Fig. 11.**  $k_D$  versus  $\langle z \rangle$  for LBQS catalogue, binning B1. The left (right) graph corresponds to the power law (exponential) parametrization.

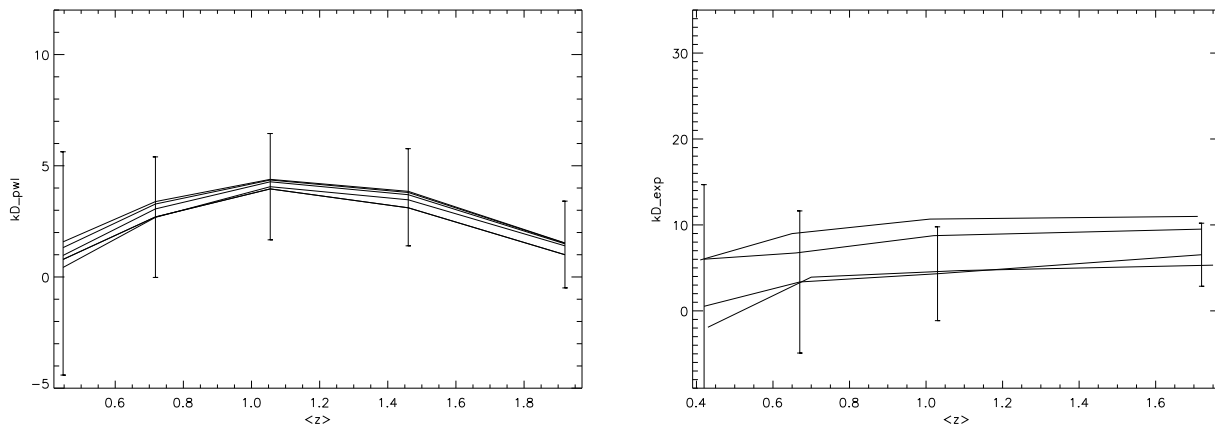


**Fig. 12.** The analysis of AAT catalogue:  $k_D$  versus  $\langle z \rangle$  for flat universe models and for binnings (B2) and (B3) given in Table 1, for the flat universe models.

## 8. Discussion

This paper presents an analysis of the evolution rate of quasars at various epochs. Our method differs from most previous ones in that it does not make use of any determination of luminosity function. It solely consists in computing the evolution parameters  $k_L$  and  $k_D$  (assuming PLE and PDE respectively) in bins of redshift, such that the  $V/V_{max}$  are uniformly distributed. However, the various selection criteria applied in the construction of the two catalogues (AAT and LBQS) as well as the different redshift and magnitude limits make a direct comparison of the results quite difficult. The method has been tested with Monte-Carlo simulated catalogues. Three binnings have been adopted, the first one with equal numbers per bin, the second and the third with a priori similar evolution rates inside each bin, according to the evolution law. Our results are the following:

- Both samples roughly show the same large trends, however modulations do appear in the LBQS results, which are likely to be correlated with the crossing of the main emission lines from the blue to the red side of the available spectral range.

- All results on the evolution parameters are quite similar whatever the hypothesis, PLE or PDE, mainly due to the inefficiency of the  $V/V_{max}$  test to distinguishing between density and luminosity evolution.

- Similar results are also obtained for both power law and exponential parametrizations. Certainly a single phenomenon cannot be described by two different laws but we note that there is no significant difference between these laws in the redshift range  $z \in [0.7, 2.2]$ , as seen in the inset plot in Fig. 13. The determination of quasars' evolution rate at high redshifts will also determine which of the proposed models is the appropriate one (if any).

- In bins with equally distributed evolution, however, both parameters  $k_L$  and  $k_D$  show far less variations with redshift and within error bars we can suppose that they are constant ( $2.5 \leq k_L \leq 4$ ,  $1.5 \leq k_D \leq 3$  in a power law parametrization).

- $k_L$  ( $k_D$ ) and  $\langle V/V_{max} \rangle$  are linearly correlated, as shown in Fig. 14.

We confirm that a PLE (or PDE) with a constant evolution parameter is a good approximation for the redshift range  $z \in [0.7, 1.7]$ . At larger redshift, the results of our analysis of the LBQS are consistent with a maximum luminosity (or density) around  $z = 2.5$ , but the reliability of these results is not yet established due to likely selection biases. The determination of this  $k(z)$  dependence towards larger  $z$  is essential for the understanding of the birth and growth of quasars at high redshifts, and the relation of the quasar phenomenon with star bursts in the primordial universe.

## Appendix

A rough estimation of the errors on  $k_L$  and  $k_D$  has been made, using the correlation we found between  $\langle V/V_{max} \rangle$  and  $k_L$  or  $k_D$  values.  $\langle V/V_{max} \rangle$  has been calculated for each bin making the hypothesis of a zero evolution.  $k_L$  versus  $\langle V/V_{max} \rangle$  is shown in Fig. 14. The dashed line and the squares correspond to binning (B1) of AAT catalogue. The dashed-dotted line and the stars correspond to AAT's binning (B2). The solid line and the triangles are the LBQS results. On the upper left we show a typical error bar on the  $\langle V/V_{max} \rangle$  estimated as  $\sigma_{\langle V/V_{max} \rangle} = (\sqrt{12N})^{-1}$ .

The coefficients of the linear approximation  $k_{L_{pwl}} = \alpha_L + \beta_L \langle V/V_{max} \rangle$  are given in Table 3 (also for  $k_D$ ), for AAT (binnings (B1) and (B2)) and LBQS. We notice that there a unique correlation may be adopted between  $k_{L_{pwl}}$  and  $\langle V/V_{max} \rangle$ , as the error bars are much more important than the variations of the coefficients  $\alpha_L$  and  $\beta_L$ . Fig. 14

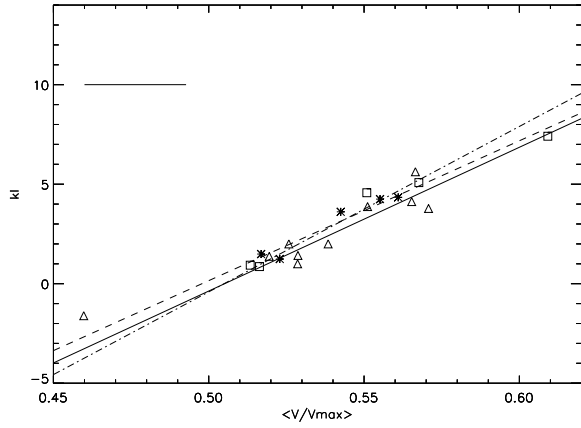


**Fig. 14.**  $k_L$  versus  $\langle V/V_{max} \rangle$  in the case of a power law parametrization. ---,  $\square$ : AAT's first binning. ---,  $*$ : AAT's second binning. —,  $\triangle$ : LBQS. All calculations have been made for the cosmological model  $(\Omega_0, \Lambda) = (0.5, 0.5)$ . In the upper-left corner, a typical error bar  $\sigma_{\langle V/V_{max} \rangle} = 1/\sqrt{12N}$ .

clearly illustrates that if the quasar population does not evolve ( $k_L$  or  $k_D = 0$ ), then their  $\langle V/V_{max} \rangle$  is equal to 0.5, as expected.

**Table 3.** Numerical values for the coefficients in the linear approximation  $k_{L_{pwl}} = \alpha_L + \beta_L \langle V/V_{max} \rangle$  and  $k_{D_{pwl}} = \alpha_D + \beta_D \langle V/V_{max} \rangle$  in a PLE and a PDE hypothesis, respectively.

Catalogue/ binning	$\alpha_L$	$\beta_L$	$\alpha_D$	$\beta_D$
AAT (B1)	-35	70.29	-22.95	47.75
AAT (B2)	-41.97	83.12	-36.74	73.08
LBQS	-36.6	72.26	-51.67	102.59

In the case of an exponential parametrization and in order to define the linear correlation, we must take under consideration the differentiation of the evolution parameters with cosmological models.

The existence of a correlation between these two quantities was somehow expected, in the sense that the higher the value of  $\langle V/V_{max} \rangle$  is under a zero evolution hypothesis, the higher  $k_L$  (or  $k_D$ ) must be in order to insure a  $\langle V/V_{max} \rangle = 0.5$  in a PLE (or PDE) hypothesis.

## References

- Boyle B. J., Fong R., Shanks T., Peterson B. A., 1988, MNRAS, 235, 935  
 Boyle B. J., Fong R., Shanks T., Peterson B. A., 1990, MNRAS, 243, 1

- Boyle B. J., Georgantopoulos I., Blair A. J., Stewart G. C., Griffiths R. E., Shanks T., Gunn K. F., Almain O., 1997, astro-ph 9710002  
 Boyle B. J., Terlevitch, R. J. 1997, astro-ph 9710134  
 Cavaliere A., Vittorini V., 1998, astro-ph 9712295  
 Goldschmidt P., Miller L., 1997, Imperial College Preprint 11  
 Guiderdoni, B., Hivon, E., Bouchet, F., Maffei, B. 1997, astro-ph 9710340  
 Haiman Z., Loeb A., 1997, astro-ph 9710208  
 Hewett P. C., Foltz C. B., Chaffee F. H., 1995, AJ, 109, 1498  
 Jones L.R., McHardy I. M., Merrifield M. R., Mason K. O., Smith P. J., Abraham R. G., Branduardi-Raymont G., Newsam A. M., Dalton G., Rowan-Robinson M., Luppino G. 1996 astro-ph 9610124  
 Krivitsky D.S., Kontorovich V.M. 1998, astro-ph 9801195  
 Lake G., Katz N., Moore B., 1997, astro-ph 9701212  
 Mathez G., Van Waerbeke L., Mellier Y., Bonnet H., Lachièze-Rey M., 1996, A&A 316, 19  
 Novosyadlyj B., Chornij Y., 1997, astro-ph 9702005  
 Page M. J., Mason K. O., McHardy I. M., Jones L. R., Carrera F. J., 1997, MNRAS, 291,324.  
 Pei Y. C., 1995, ApJ, 438,623  
 Schmidt M., 1968, ApJ, 151, 393  
 Schmidt M., Green R. F., 1983, ApJ, 269, 352  
 Schmidt M., Schneider D. P., Gunn J. E., 1995, AJ, 110, 68  
 Shaver P. A., 1994, *17th Texas Symposium on Relativistic Astrophysics and Cosmology*  
 Shaver P. A., Hook J. M., Jackson C. A., Wall J. V., Kellermann K. I., 1998, astro-ph/9801211  
 Siemiginowska A., Elvis M., 1997, ApJ, 482, L9  
 Smail, I., Ivison, R. J., Blain, A. W. 1997, astro-ph 9708135  
 Ulrich M. H., 1989, A&A, 220, 71  
 Van Waerbeke L., Mathez G., Mellier Y., Bonnet H., Lachièze-Rey M., 1996, A&A, 316, 1  
 Warren S. J., Hewett P. C., Osmer P. S. 1994 ApJ, 421, 412  
 Yi I., 1996, ApJ, 473, 645